



Forms of phosphate occurrences observed in cathodoluminescence: Cambrian of the Polish part of the East European Craton

Magdalena SIKORSKA



Sikorska M. (1998) — Forms of phosphate occurrences observed in cathodoluminescence: Cambrian of the Polish part of the East European Craton. *Geol. Quart.*, 42 (1): 15–28. Warszawa.

Cambrian rocks of the Polish part of the East European Craton contain numerous occurrences of phosphates. Their diversity was delineated due to cathodoluminescence (CL) study. Two categories of phosphates were recognised in the studied rocks: (I) redeposited phosphates and (II) diagenetic phosphates. Within these two categories different types of phosphate occurrences were distinguished. During the early stage of diagenesis, pore solutions are enriched in phosphorus which allows precipitation of calcium phosphate in pores, on the grain surface or inside the pseudomorphs.

Magdalena Sikorska, Polish Geological Institute, ul. Rakowiecka 4, 00-975 Warszawa, Poland (received: 04.12.1997; accepted: 09.01.1998).

INTRODUCTION

Occurrence of phosphates in the Cambrian sediments in Poland has been reported since early thirties. The main interest, however, was directed towards nodules and concretions together described as phosphorites. Their presence in the Cambrian rocks was (for the first time) noted in the Góry Pieprzowe Mts. (R. Kozłowski, 1931) and in the sediments of the East European Craton — initially in deep boreholes from Podlasie region (K. Lenzion, 1968).

Occurrence of phosphorites is also known from the neighbouring countries. They were described from the Cambrian of western Belarus (V. I. Abramenko *et al.*, 1992) and from southern part of Scandinavia (M. D. Brasier, 1980; B. Wallin, 1982). Worth mentioning is also occurrence of primary phosphatic oolites in the Cambrian sandstones from Spitsbergen (K. Swett, R. K. Crowder, 1982). Economic size concentrations of Cambrian phosphorite-bearing sediments are also known from SE Asia, Australia and — to lesser extent — from eastern part of Canada and Western Europe (M. D. Brasier, 1980).

Rock samples described in this publication come from 12 deep boreholes (Fig. 1). In the area studied, i.e. in the Polish part of the East European Craton, the depth of bottom surface of Cambrian sediments ranges from around 1070 m in the NE portion, to about 5400 m in the SW portion.

RESEARCH METHODS

After an initial petrographic examination under the polarising microscope, cathodoluminescence study was conducted on 30 thin sections. It was performed with an aid of Nikon microscope *Optiphot 2* linked with *Cambridge Image Technology Ltd.* cathodoluminescence unit *CCL 8200 mk3*. Applied voltage ranged between 12 and 15 kV and the intensity of beam current was about 500 μ A. Photographs were taken on a *Fuji* film 1600 ASA.

Phenomenon of cathodoluminescence involves emission of light by minerals under excitation by an electron beam (U. Zinkernagel, 1978). Brightness and colour of induced in such

microscopic analysis (Pl. I, Fig. 9), but CL image shows clear relicts of largely phosphatised K-feldspar (Pl. I, Fig. 10).

In the case of phosphate grains composed exclusively of phosphatic matter, the establishing of their provenance is difficult. Such grains may represent either phosphatised feldspars, phosphatised grains of glauconite or fecal pellets. Although the presence of the fecal pellets can not be excluded, it is rather unlikely. Only very rarely phosphatised grains have rod-like shape characteristic for the fecal pellets (Pl. II, Fig. 11). Microprobe (EDS) analyses of chemical composition of such grain indicated that it contains apatite and aluminosilicate chemically consistent with illite (Fig. 2).

In the case of phosphatisation of glauconite in the Cambrian rocks different stages of this process can be observed. CL images reveal glauconite grains with single crystals of apatite (Pl. II, Figs. 13 and 14) as well as phosphatised grains having form and size indicating their primary glauconitic composition (Pl. II, Fig. 12). Quantitative microprobe (EDS) analyses of such grains indicated that they are composed predominantly of fluorapatite (2.6% F) and minor amounts of aluminosilicate showing composition consistent with glauconite. G. R. Birch (1979) described similar grains of glauconite containing concentrations of phosphates from recent rocks in shelf sediments in South Africa. The author named them "variegated pellets" and associated their development with the earliest stage of formation of glauconite.

The examples given above indicate that caution should be exercised while drawing genetic conclusions based on identification of phosphate grains under standard polarising microscope. Additional CL observations are necessary to establish provenance of such grains.

Similarly, process of phosphatisation of micas is best visible on CL images. Here a good example is image shown on Plate II, Figures 15 and 16. Difficult to identify under a standard microscope dark pigment between mica blades exhibits luminescence characteristic for phosphates. In addition, calcite lamellae present inside partly carbonatised mica packet are clearly visible due to their orange luminescence colour. Microprobe (EDS) qualitative analyses confirmed presence of fluorapatite and calcite between the blades of mica.

Figure 3 shows a map of Al, P and Ca content in this mica grain illustrating distribution of three earlier mentioned mineral phases.

Bioclasts (Pl. III, Fig. 17) require a separate mention among the phosphate occurrences. In the case of studied Cambrian rocks, the bioclasts comprised fragments of phosphate inarticulate brachiopods or phosphatised skeletons of trilobites. Some of such bioclasts become completely silicified during later diagenetic stages and only their contours are visible.

PHOSPHATE RIMS

Grain framework of the Cambrian sandstones contains detrital grains (mostly quartz, but also feldspar and heavy minerals) with phosphate rims. Most often they are single

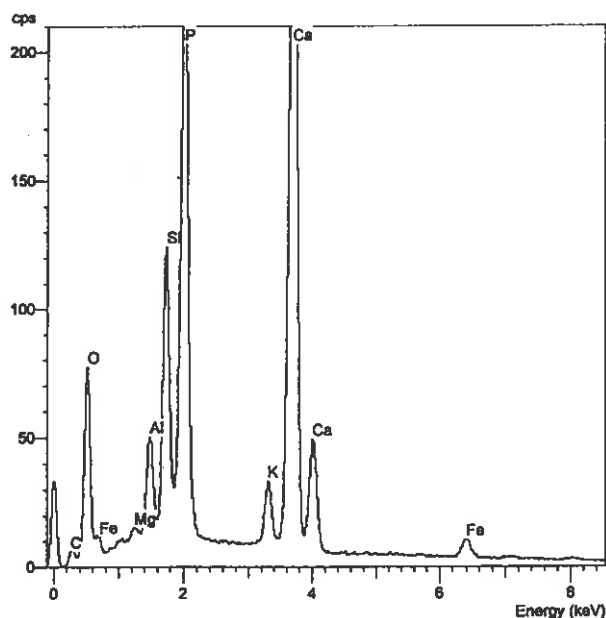


Fig. 2. Diagram of qualitative microprobe (EDS) analysis of a phosphate grain (fecal pellet) presented on Plate II, Figure 11. The grain is composed of calcium phosphate and illite. Borehole Kościerzyna IG 1, depth 4714.8 m

Wykres punktowej analizy jakościowej (EDS) ziarna fosforanowego (grudki fekalnej) przedstawionego na tabl. II, fig. 11. W skład ziarna wchodzi fosforan wapnia oraz illit. Kościerzyna IG 1, głęb. 4714,8 m

grains visible in thin section (Pl. II, Fig. 11), but in some cases all grains in the rock have phosphate rims (boreholes: Darżlubie IG 1, depth 3281.7 m; Łopiennik IG 1, depth 4461.2 m). In the latter case (Pl. III, Fig. 18) the rims occur along grain contacts indicating their development before mechanical compaction, i.e. during an early diagenetic stage.

Phosphatic rims can be regularly developed over the whole grain surface (Pl. V, Fig. 29) but often they occur in fragments, are broken or deformed during the process of formation of quartz overgrowths. Very often phosphate rims are completely silicified. The thickness of rims usually ranges between 0.005 and 0.01 mm (occasionally reaches 0.03 mm); but they also can be very thin, barely seen under the microscope. Particularly in such cases CL research, which can detect rims as thin as 0.001 mm, is useful. Scanning microscope (SEM) observations indicated that colophane rims, homogeneously looking under the polarising microscope, are — in fact — composed of microcrystalline apatite showing columnar structure (Pl. V, Figs. 30 and 31). Microprobe (EDS) qualitative chemical analyses revealed that such rims are composed of fluorapatite (Fig. 4).

APATITE CRYSTALS

Another type of phosphate occurrences are small crystals of apatite present inside pseudomorphs after K-feldspars and on the primary surfaces of quartz grains. Such crystals vary

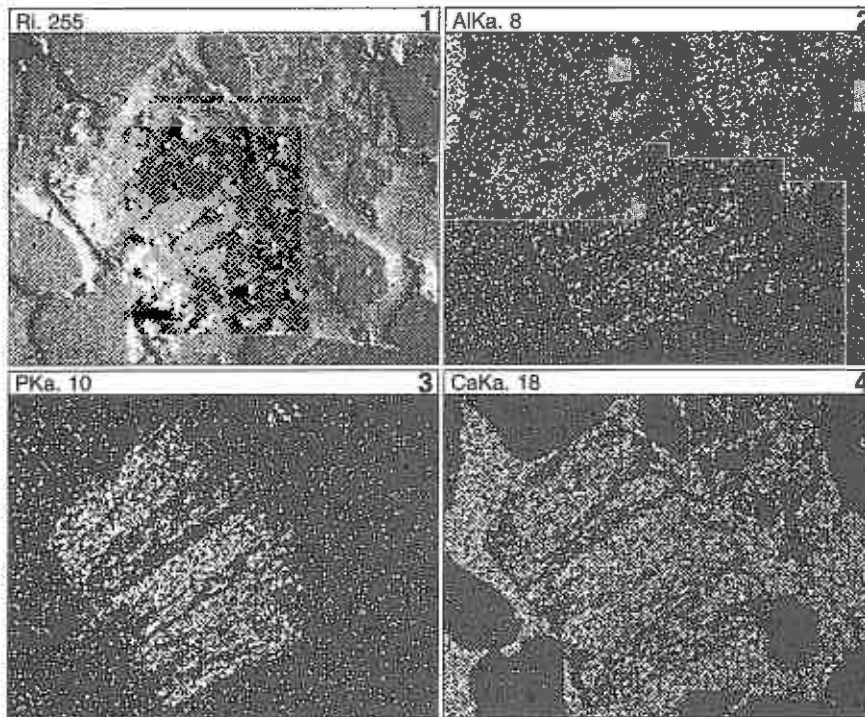


Fig. 3. Map of aluminium, phosphorus and calcium content in partly carbonatised and phosphatised mica
 1 — BEI image of mica; 2 — map for Al; 3 — map for P; 4 — map for Ca (see also Pl. II, Figs. 15 and 16); borehole Łopiennik IG 1, depth 5392.1 m
 Mapy rozkładu zawartości glinu, fosforu i wapnia w łyszczyku, który uległ częściowej karbonatyzacji i fosfatyzacji
 1 — obraz BEI łyszczyku; 2 — mapa dla Al; 3 — mapa dla P; 4 — mapa dla Ca (patrz tabl. II, fig. 15 i 16); Łopiennik IG 1, głęb. 5392,1 m

in size from 0.005 to 0.04 mm. They usually form concentrations or, less frequently, occur as isolated crystals. The latter were noted in strongly silicified sandstone (borehole Słupsk IG 1, depth 4974.3 m) inside quartz pseudomorphs after K-feldspars (Pl. III, Figs. 19 and 20).

Identification of apatite and conclusion that the original mineral was feldspar is often possible only basing on the CL images. CL images also reveal zonation in some apatite crystals. In the sandstone samples from borehole Busówno IG 1 authigenic apatite forms concentrations of minute crystals

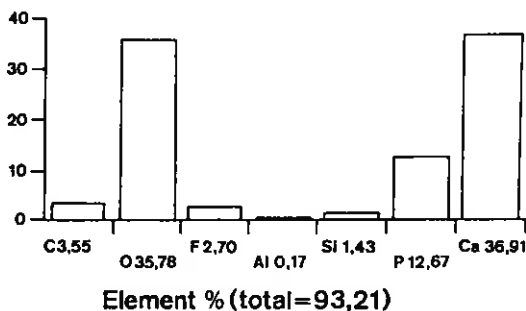


Fig. 4. Results of microprobe (EDS) analysis of phosphate rim on a grain of quartz (see Pl. II, Fig. 11). The rim consists of fluorapatite. Borehole Kościerzyna IG 1, depth 4714.8 m

Wyniki punktowej analizy ilościowej (EDS) otoczki fosforanowej na ziarnie kwarcu (patrz tabl. II, fig. 11). Otoczka składa się z fluoroapatytu. Kościerzyna IG 1, głęb. 4714,8 m

within argillised and sometimes partly silicified crystals of K-feldspars (Pl. III, Fig. 21). Quartz-apatite pseudomorphs after K-feldspars were also observed in Cambrian sandstones from borehole Białogóra 6 and from offshore boreholes at the Baltic Sea (M. Sikorska, 1997).

Another type of apatite-bearing pseudomorphs after feldspars are carbonatised grains of K-feldspars. A standard microscopic image of sandstone from borehole Darżlubie IG 1 (depth 3281.7 m) shows carbonate cement (Pl. IV, Fig. 23), while CL image (Pl. IV, Fig. 24) exposes, in the same place, feldspar relicts as well as small concentrations and singular crystals of apatite. Phosphates are placed inside a grain and form a rim around it, clearly indicating the original shape of carbonatised feldspar.

In a sample from borehole Gdańsk IG 1 (depth 3363.7 m) crystals of apatite are present around perfectly rounded quartz grains, which are surrounded by a subtle film of phosphate. It is particularly well exposed on CL images (Pl. III, Fig. 22). It can be also observed that singular apatite crystals are also emplaced in quartz cement.

CL research allowed identification of disseminated phosphates in the muddy matrix of sandstones (Pl. IV, Figs. 25 and 26) as well as in the mudstones themselves. Very fine (0.005 to 0.01 mm in size) concentrations of phosphates, due to their milky luminescence colours, are easily visible on a dark background of clay minerals and silty quartz detritus. Scanning microscope analyses indicated, that apatite forms single crystals or aggregates of several columnar crystals (Pl. V, Fig. 32).

OOIDS

No primary phosphatic ooids were found in the studied Cambrian rocks. Occasionally other types of ooids were observed including chamositic, ferruginous and calcitic (boreholes Gdańsk IG 1 and Hel IG 1). In a sample from borehole Gdańsk IG 1 (depth 3363.7 m) partly phosphatised chamositic ooids with concentric rings of fine apatite crystals were recognised (Pl. IV, Fig. 27).

PHOSPHATE CEMENT

In single cases, phosphate cement was observed in the studied Cambrian sandstones (Pl. IV, Fig. 28). It forms nest-shaped concentrations in the rocks with regenerative quartz cement. The phosphate forms rims with radial internal structure around grains. Composition and texture of detrital material cemented by phosphate is identical with the rest of the rock suggesting diagenetic origin of such nest-shaped phosphate concentrations.

ORIGIN OF PHOSPHATE OCCURRENCES

It is beyond doubt that the origin of phosphate lithoclasts (phosphorite pebbles) present in the studied Cambrian sandstones differs from provenance of other occurrences of phosphate. It is widely accepted that phosphorite rocks form on a shelf during slow or periodically completely stopped deposition (B. Wallin, 1982). During transgressive/regressive (and opposite) cycles, the bottom sediment is extensively reworked by storms and is transported to other parts of a sedimentary basin.

Such process leads to development of phosphate clasts located in mineralogically and texturally mature sands on a shelf and shore zone. The redeposited material also includes part of phosphatic organic detritus. In such case it is difficult to establish whether phosphatisation of primarily carbonate bioclasts took place before or after the redeposition.

Contrary to phosphate lithoclasts (phosphorite pebbles) and to phosphate bioclasts, other types of phosphates are diagenetic, associated with post-sedimentary processes in the host rocks.

There are several theories explaining provenance of phosphorus in the sea water. It can, for example, be delivered from land with weathering material transported by rivers (P. S. Balson, 1980; U. Stuesson, H. Bauert, 1994). The main source of phosphorus in the sea water is, however, organic detritus. Intensive development of marine organisms is possible, among the other factors, due to ascending currents delivering large amounts of nutrients from the deeper parts of the basin (B. Wallin, 1982).

Significant enrichment in phosphorus takes place in the pore waters of freshly deposited sediment. In theory, three

processes can be responsible for such enrichment (J. H. S. Macquaker, K. G. Taylor, 1996; B. Rasmussen, 1996): (1) dissolution of skeletons of marine organisms; (2) decomposition of organic matter; (3) liberation of phosphorus from iron oxides. Near the sediment/water interface iron oxides adsorb fluorine from the sea water and phosphorus from the decaying organic matter. As a result of iron reduction after burial of the sediment, both these elements (fluorine and phosphorus) are liberated into the pore waters.

There is no consensus, however, between the researchers, whether crystallisation of apatite from the pore waters occurs directly, or whether phosphate gel is precipitated firstly (M. Slansky, 1980).

Occurrence of apatite in pseudomorphs after K-feldspars suggests a possibility of existence of additional source of phosphorus in the studied rocks. According to the latest studies (D. London, 1992; J. Fryda, K. Breiter, 1995) feldspars could contain up to 2.5 wt% P₂O₅ therefore, could possibly be a source of phosphorus themselves. Phosphorus and aluminium substitute silica in the crystal lattice of feldspars: Al³⁺ + P⁵⁺ = Si⁴⁺ + Si⁴⁺. Phosphorus released during the process of feldspar dissolution can be in such a case a source of phosphate crystals developing in pseudomorphs after feldspars.

There are substantial research data indicating an important role played by bacteria in the phosphatisation process (R. D. A. Smith, 1987; A. Kühn, K. Radlicz, 1988; B. Rasmussen, 1996). A. Kühn and K. Radlicz (1988) observed in Cambrian rocks under electron microscope spheric structures similar to bacteria.

Another process taking place in the zone near sediment/water interface is an absorption of rare earth elements (REE) by biogenic apatite (J. Wright *et al.*, 1987). This process occurs shortly after the deposition and reflects presence of these elements in the sea water. The presence of REE in phosphates causes their luminescence and, therefore, enables their identification on CL images.

SUMMARY AND CONCLUSIONS

Summarising the review of types of phosphate occurrences in the Cambrian rocks of the Polish part of the East European Craton, an attempt was undertaken to classify such occurrences. Described occurrences of phosphate were divided into two principal groups: redeposited phosphates and diagenetic phosphates.

The redeposited phosphates include phosphate lithoclasts (phosphorite pebbles) transported from other parts of a sedimentary basin and phosphate bioclasts. Such grains comprise majority of phosphates classified by some researchers as "phosphoclasts", which include also phosphatised bioclasts.

The diagenetic phosphates comprise rock components which were partly or completely phosphatised. They include earlier mentioned phosphatised bioclasts and phosphatised mineral grains (feldspars, glauconite, micas), fecal pellets and ooids. In addition, diagenetic phosphates include phosphate

rims and apatite crystals occurring on detrital grains, in pseudomorphs after feldspars as well as in silty-clay matrix and phosphate cement.

On the basis of the above comments the studied Cambrian phosphates can be classified as follows:

I — redeposited phosphates: phosphate lithoclasts (= phosphorite pebbles) and phosphate bioclasts;

II — diagenetic phosphates: phosphatised bioclasts, phosphatised mineral grains, phosphatised fecal pellets, phos-

phatised ooids, phosphate rims, apatite crystals and phosphate cement.

A particular role of cathodoluminescence studies has to be highlighted. Such studies allow to easily delineate different forms of phosphate occurrences in the rocks. This method is very important in identification of phosphates of diagenetic provenance.

Translated by Andrzej Wygralak and Magdalena Sikorska

REFERENCES

- ABRAMENKO V. I., ZINOVENKO G. V., PISKUN L. V. (1992) — Reference sections and lithostratigraphy of the Cambrian and Vendian deposits in the Podlasie–Brest Depression. *Prz. Geol.*, **40**, p. 69–77, no. 2.
- BALSON P. S. (1980) — The origin and evolution of Tertiary phosphorites from eastern England. *J. Geol. Soc.*, **137**, p. 723–730, no. 6.
- BIRCH G. F. (1979) — The nature and origin of mixed apatite/glaucinite pellets from the continental shelf of South Africa. *Mar. Geol.*, **29**, p. 313–334, no. 1/4.
- BRASIER M. D. (1980) — The Lower Cambrian transgression and glauconite-phosphate facies of western Europe. *J. Geol. Soc.*, **137**, p. 695–704, no. 6.
- FRYDA J., BREITER K. (1995) — Alkali feldspars as a main phosphorus reservoirs in raremetal granites: three examples from the Bohemian Massif (Czech Republic). *Terra Nova*, **7**, p. 315–320, no. 3.
- JAWOROWSKI K. (1986) — Sedymentacja osadów wendy i kambry. *Helig 1. Profile Głęb. Otw. Wiertn. Inst. Geol.*, **63**, p. 129–143.
- JAWOROWSKI K. (1997) — Depositional environments of the Lower and Middle Cambrian sandstone bodies; Polish part of the East European Craton (in Polish with English summary). *Biul. Państw. Inst. Geol.*, **377**.
- KARAKUS M., HAGNI R. D., SPRENG A. C. (1996) — Cathodoluminescence petrography of the phosphate grains in the Lower Jurassic (Aalenian) ironstones of Lorraine, France. *Intern. Conf. "Cathodoluminescence and related techniques in geosc. and geomaterials"*. Abstracts, p.71–72. Nancy, France.
- KOZŁOWSKI R. (1931) — Fosforyty w utworach kambryjskich Sandomierza. *Pos. Nauk. Państw. Inst. Geol.*, **30**, p. 61.
- KÜHN A., RADLICZ K. (1988) — Nanostructures of phosphorite cement and bacteria-like features in phosphorite conglomerate of the Pieprzowe Mts. (in Polish with English summary). *Prz. Geol.*, **36**, p. 502–507, no. 9.
- LENDZION K. (1968) — Kambryjska północno-wschodnia. In: *Budowa geologiczna Polski, part 1 — Stratygrafia*, p. 137–180.
- LONDON D. (1992) — Phosphorus in S-type magmas: The P₂O₅ content of feldspars from peraluminous granites, pegmatites, and rhyolites. *Amer. Miner.*, **77**, p. 126–145, no. 1/2.
- MACQUAKER J. H. S., TAYLOR K. G. (1996) — A sequence — stratigraphic interpretation of a mudstone — dominated succession: the Lower Jurassic Cleveland Ironstone Formation, UK. *J. Geol. Soc.*, **153**, p. 759–770, no. 5.
- RASMUSSEN B. (1996) — Early diagenetic REE — phosphate minerals (florencite, gorceixite, crandallite and xenotime) in marine sandstones: A major sink for oceanic phosphorus. *Amer. J. Sc.*, **296**, no. 6.
- SIKORSKA M. (1997) — Petrografia skał kambryjskich. In: *Ocena perspektyw poszukiwawczych złóż ropy naftowej i gazu ziemnego w utworach kambryjskich perybałtyckiej na podstawie analizy basenów sedymentacyjnych starszego paleozoiku*. *Centr. Arch. Geol. Państw. Inst. Geol. Warszawa*.
- SLANSKY M. (1980) — Geologie de phosphates sedimentaires. *Mem. BRGM*, **114**.
- SMITH R. D. A. (1987) — Early diagenetic phosphate cements in a turbidite basin. In: *Diagenesis of sedimentary sequence* (ed. J. D. Marshall). *Geol. Soc. Spec. Publ.*, **36**, p. 141–156.
- STURESSON U., BAUERT H. (1994) — Origin and palaeogeographical distribution of the Viruan iron and phosphate ooids in Estonia: evidence from mineralogical and chemical compositions. *Sed. Geol.*, **93**, p. 51–72, no. 1/2.
- SWETT K., CROWDER R. K. (1982) — Primary phosphatic oolites from the Lower Cambrian of Spitsbergen. *J. Sed. Petrol.*, **52**, p. 587–594, no. 2.
- WALLIN B. (1982) — Sedimentology of the Lower Cambrian sequence at Vassbo, Sweden. *Stockholm Contr. Geol.*, **39**, no. 1.
- WRIGHT J., SCHRADER H., HOLSER W. T. (1987) — Paleoredox variations in ancient oceans recorded by rare earth elements in fossil apatite. *Geochim. Cosmochim. Acta*, **51**, p. 631–644, no. 3.
- ZINKERNAGEL U. (1978) — Cathodoluminescence of quartz and its application to sandstone petrology. *Contr. Sed.*, **8**.

FORMY WYSTĘPOWANIA FOSFORANÓW W SKAŁACH KAMBRYJSKICH OBSERWOWANE W KATODOLUMINESCENCJI (POLSKA CZĘŚĆ PLATFORMY WSCHODNIOEUROPEJSKIEJ)

Streszczenie

W skałach kambryjskich polskiej części platformy wschodnioeuropejskiej stwierdzono liczne fosforany. Ich różnorodność została ujawniona w płytkach cienkich badanych w katodoluminescencji (CL). Wzbudzenie wiązką elektronów wywołuje w fosforanach silną luminescencję w barwach od mlecznobiałej przez mlecznożółtą do bładoróżowej, bładoniebieskiej i niekiedy mlecznozarej. Pierwiastkami wywołującymi to świecenie są: mangan oraz pierwiastki ziem rzadkich (M. Karakus i in., 1996). Fosforany występujące w badanych skałach podzielono na dwie zasadnicze kategorie: redeponowane i diagenetyczne.

Do fosforanów redeponowanych zaliczono przyniesione z innych części zbiornika litoklasty fosforanowe (okruchy skał fosforytowych) oraz fosforanowe bioklasty. Ziarna te stanowią podstawową część wyróżnianej przez niektórych badaczy kategorii fosforanów określanej mianem fosfoklastów, do których należą także sfosfatyzowane bioklasty.

Do fosforanów pochodzenia diagenetycznego zaliczono składniki skał, które uległy częściowej lub całkowitej sfosfatyzacji. Należą tu, wspomniane wcześniej, sfosfatyzowane bioklasty oraz sfosfatyzowane ziarna mineralne (skalanie, glaukonit, tyszczki), grudki fekalne i ooidy. Ponadto w grupie fosforanów diagenetycznych znalazły się otoczki fosforanowe oraz kryształki

apatytu, obecne na ziarnach detrytycznych, w pseudomorfozach po skałkach i w matriksie ilasto-pylastym, oraz cement fosforanowy.

Jak wynika z powyższych uwag, zbadane fosforany kambryjskie można sklasyfikować następująco: (I) fosforany redeponowane: litoklasty fosforanowe (= okruchy fosforytowe) i bioklasty fosforanowe; (II) fosforany diagenetyczne: sfosfatyzowane bioklasty, sfosfatyzowane ziarna mineralne,

sfosfatyzowane grudki fekalne, sfosfatyzowane ooidy, otoczki fosforanowe, kryształy apatyty i cement fosforanowy.

Na szczególne podkreślenie zasługuje rola badań katodoluminescencyjnych, które pozwalają w bardzo prosty sposób ujawnić różne formy istnienia fosforanów w skale. Metoda ta ma ogromne znaczenie w przypadku identyfikacji fosforanów pochodzenia diagenetycznego.

EXPLANATIONS OF PLATES

XP — microscopic image, crossed polars; PL — microscopic image, plane polarised light; CL — cathodoluminescence image (XP and CL image couples show the same fragment of thin section); SEM — scanning electron microscope image

XP — zdjęcie mikroskopowe, nikole skrzyżowane; PL — zdjęcie mikroskopowe, bez analizatora; CL — zdjęcie katodoluminescencyjne (pary zdjęć XP i CL przedstawiają ten sam fragment płytki cienkiej); SEM — zdjęcie ze skaningowego mikroskopu elektronowego

PLATE I

Figs. 5, 6. XP — quartz arenite with abundant glauconite. On the left barely seen phosphate lithoclast (L) (Fig. 5). CL — clearly seen sandy phosphate lithoclast (L) (milky-white luminescence colour of phosphate). Note two grains in contact with phosphate rim (arrow) in the lower right corner (Fig. 6). Borehole Kościerzyna IG 1, depth 4714.8 m

XP — arenit kwarcowy z dużą ilością glaukonitu. Z lewej strony słabo widoczny litoklast fosforanowy (L) (fig. 5). CL — wyraźnie widoczny piaszczysty litoklast fosforanowy (L) (mlecznobiała barwa luminescencji fosforanu). W prawym dolnym rogu dwa stykające się ziarna z otoczkami fosforanowymi (strzałka) (fig. 6). Kościerzyna IG 1, głęb. 4714,8 m

Fig. 7. CL — fragment of sandy phosphate lithoclast. Phosphate forms rims around grains (grey luminescence colour) and partly replaces them (milky-pink luminescence colour). Calcitic cement (c) fills pore spaces and replaces some grains. Borehole Łopiennik IG 1, depth 5392.1 m

CL — fragment piaszczystego litoklastu fosforanowego. Fosforan tworzy otoczki wokół ziarn (szara barwa luminescencji) oraz częściowo je zastępuje (mlecznoróżowa barwa luminescencji). Cement kalcytowy (c) wypełnia przestrzeń porową oraz zastępuje niektóre ziarna. Łopiennik IG 1, głęb. 5392,1 m

Fig. 8. CL — grain of K-feldspar (blue luminescence colour) phosphatised along the cleavage planes (light brown luminescence colour). Borehole Okuniew IG 1, depth 4235.8 m

CL — ziarno skalenia potasowego (niebieska barwa luminescencji), w którym wzdłuż płaszczyzn łupliwości nastąpiła fosfatyzacja (jasnobrązowa barwa luminescencji). Okuniew IG 1, głęb. 4235,8 m

Figs. 9, 10. XP — two phosphate grains in quartz arenite (Fig. 9). CL — one of the phosphate grains (F) represent phosphatised K-feldspar; relicts of K-feldspar are visible only on CL image (blue luminescence colour) (Fig. 10). Borehole Okuniew IG 1, depth 4235.8 m

XP — dwa ziarna fosforanowe w arenicie kwarcowym (fig. 9). CL — jedno z ziarn fosforanowych (F) jest sfosfatyzowanym skałkiem potasowym, którego relikty widoczne są jedynie na obrazie CL (niebieska barwa luminescencji) (fig. 10). Okuniew IG 1, głęb. 4235,8 m

PLATE II

Fig. 11. CL — rod-shaped phosphate grain (F) characteristic for fecal pellets. Nearby quartz grain with rim of phosphate. For microprobe (EDS)

chemical analysis of phosphate grain and phosphate rim see Figs. 2 and 4. Borehole Kościerzyna IG 1, depth 4714.8 m

CL — ziarno fosforanowe (F) o walczkowatym kształcie charakterystycznym dla grudek fekalnych. Obok ziarno kwarcu z otoczką fosforanową. Analiza składu chemicznego (EDS) ziarna fosforanowego na fig. 2 oraz otoczki fosforanowej na fig. 4. Kościerzyna IG 1, głęb. 4714,8 m

Fig. 12. CL — variably phosphatised (milky-pink luminescence colour) grains of glauconite (g). Borehole Kościerzyna IG 1, depth 4714.8 m

CL — ziarna glaukonitu (g) w różnym stopniu sfosfatyzowane (mlecznoróżowa barwa luminescencji). Kościerzyna IG 1, głęb. 4714,8 m

Figs. 13, 14. XP — grain of glauconite (g) in quartz arenite (Fig. 13). CL — small crystals of apatite (milky-white luminescence colour) disseminated in the glauconite grain. Initial phase of phosphatisation of glauconite (Fig. 14). Borehole Prabuty IG 1, depth 3792.4 m

XP — ziarno glaukonitu (g) w arenicie kwarcowym (fig. 13). CL — w ziarnie glaukonitu widoczne rozszanie drobne kryształy apatyty (mlecznobiała barwa luminescencji). Początkowa faza fosfatyzacji glaukonitu (fig. 14). Prabuty IG 1, głęb. 3792,4 m

Figs. 15, 16. XP — carbonatised quartz arenite. In the centre partly carbonatised mica (Ł) covered by brown pigment (Fig. 16). CL — mica blades partly replaced by calcite (yellow-orange luminescence colour), partly phosphatised (arrow) and partly unaltered (black — no luminescence) (Fig. 16). Borehole Łopiennik IG 1, depth 5392.1 m

XP — skarbonatyzowany arenit kwarcowy. W centrum lyszczki (Ł) częściowo skarbonatyzowany, pokryty brunatnym pigmentem (fig. 15). CL — część blaszek lyszczki zastąpiona kalcytem (żółtopomarańczowa barwa luminescencji), część sfosfatyzowana (strzałka), a część nie zmieniona (czarna barwa — brak luminescencji) (fig. 16). Łopiennik IG 1, głęb. 5392,1 m

PLATE III

Fig. 17. CL — phosphate bioclast (b) — fragment of brachiopod shell showing layered structure. Borehole Darżlubie IG 1, depth 3015.0 m

CL — bioklast fosforanowy (b) — fragment skorupki brachiopodowej o widocznej budowie warstwowej. Darżlubie IG 1, głęb. 3015,0 m

Fig. 18. CL — quartz grains with thin phosphate rims (milky-white luminescence colour). Quartz cement (q). Borehole Darżlubie IG 1, depth 3281.7 m

CL — ziarna kwarcu z cienkimi otoczkami fosforanowymi (mlecznobiała barwa luminescencji). Cement kwarcowy (q). Darżlubie IG 1, głęb. 3281,7 m

Figs. 19, 20. XP — quartz pseudomorph (ps) after feldspar with singular crystals of apatite (arrows) (Fig. 19). CL — relicts of K-feldspar (blue luminescence colour) and apatite crystals (milky-pink luminescence colour). Weak zonation of apatites can be observed (Fig. 20). Borehole Słupsk IG 1, depth 4974.3 m

XP — pseudomorfoza kwarcowa (ps) po skałeniu z pojedynczymi kryształami apatyty (strzałki) (fig. 19). CL — relikty skalenia potasowego (niebieska barwa luminescencji) i kryształy apatyty (mle-

cznoróżowa barwa luminescencji). Słabo widoczna budowa pasowa w apatytach (fig. 20). Słupsk IG 1, głęb. 4974,3 m

Fig. 21. CL — quartz-illite pseudomorph after feldspar (arrow) with minute crystals of apatite (milky-white luminescence colour). Borehole Busówno IG 1, depth 3581.5 m

CL — pseudomorfoza kwarcowo-ilasta po skaleniu (strzałka) z drobnymi kryształami apatytu (mlecznobiała barwa luminescencji). Busówno IG 1, głęb. 3581,5 m

Fig. 22. CL — crystals of apatite (milky-white luminescence colour) around quartz grains. Quartz cement (q). Borehole Gdańsk IG 1, depth 3363.7 m

CL — kryształy apatytu (mlecznobiała barwa luminescencji) wokół ziarn kwarcu. Cement kwarcowy (q). Gdańsk IG 1, głęb. 3363,7 m

XP — mułowcowy matrix w piaskowcu (fig. 25). CL — rozproszone drobne kryształy apatytu w matryksie mułowcowym (fig. 26). Darżlubie IG 1, głęb. 3333,8

Fig. 27. CL — Partly phosphatised chamositic ooid. Apatite crystals (milky-white luminescence colour) aligned conformably to concentric zones of cortex. Subtle rims of phosphates visible on quartz grains. Borehole Gdańsk IG 1, depth 3363.7 m

CL — sfosfatyzowany częściowo ooid szamozytowy. Widoczne kryształy apatytu (mlecznobiała barwa luminescencji) ułożone zgodnie z koncentrycznymi powłokami korteksu. Na ziarnach kwarcu subtelne otoczki fosforanowe. Gdańsk IG 1, głęb. 3363,7 m

Fig. 28. PL — phosphate cement (cf) in quartz arenite. Borehole Busówno IG 1, depth 3581.5 m

PL — cement fosforanowy (cf) w arenicie kwarcowym. Busówno IG 1, głęb. 3581,5 m

PLATE IV

Figs. 23, 24. XP — ankerite cement (a) in quartz arenite (Fig. 23). CL — in the centre ankerite pseudomorph after K-feldspar. Inside the pseudomorph feldspar relicts (blue luminescence colour) and minute concentrations of phosphate (milky-white luminescence colour) can be seen. Fragments of preserved phosphate rim (arrows) on the primary feldspar. Nearby a grain of quartz (Q) with distinct rim of phosphates (Fig. 24). Borehole Darżlubie IG 1, depth 3281.7 m

XP — cement ankerytowy (a) w arenicie kwarcowym (fig. 23). CL — w centrum pseudomorfoza ankerytowa po skaleniu potasowym. Widoczne relikty skalenia (niebieska barwa luminescencji) oraz drobne skupienia fosforanowe (mlecznobiała barwa luminescencji) wewnątrz pseudomorfozy. Fragmentarycznie zachowana otoczka fosforanowa (strzałki) na pierwotnie istniejącym skaleniu. Obok ziarno kwarcu (Q) z wyraźną otoczką fosforanową (fig. 24). Darżlubie IG 1, głęb. 3281,7 m

Figs. 25, 26. XP — mudstone matrix in sandstone (Fig. 25). CL — disseminated minute crystals of apatite (milky-white luminescence colour) in mudstone matrix can be observed (Fig. 26). Borehole Darżlubie IG 1, depth 3333.8 m

PLATE V

Fig. 29. SEM — quartz grain coated with phosphate. Borehole Terebin IG 5, depth 3075.8 m

SEM — ziarno kwarcu z powłoką fosforanową. Terebin IG 5, głęb. 3075,8 m

Fig. 30. SEM — phosphate rim (arrow) around a quartz grain. Borehole Łopiennik IG 1, depth 4461.2 m

SEM — otoczka fosforanowa (strzałka) wokół ziarna kwarcu. Łopiennik IG 1, głęb. 4461,2 m

Fig. 31. SEM — fragment of phosphate rim with visible columnar crystals of apatite. Borehole Łopiennik IG 1, depth 4461.2 m

SEM — fragment otoczki fosforanowej z widocznym słupkowym pokrojem kryształów apatytu. Łopiennik IG 1, głęb. 4461,2 m

Fig. 32. SEM — columnar apatite (A) in clay matrix (compare Figs. 25 and 26). Borehole Darżlubie IG 1, depth 3333.8 m

SEM — apatyt (A) o pokroju słupkowym tkwiący w masie ilastej (por. fig. 25 i 26). Darżlubie IG 1, głęb. 3333,8 m

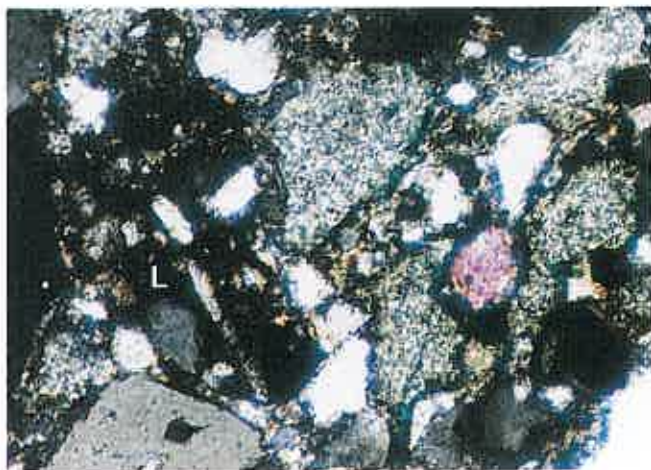


Fig. 5



Fig. 6

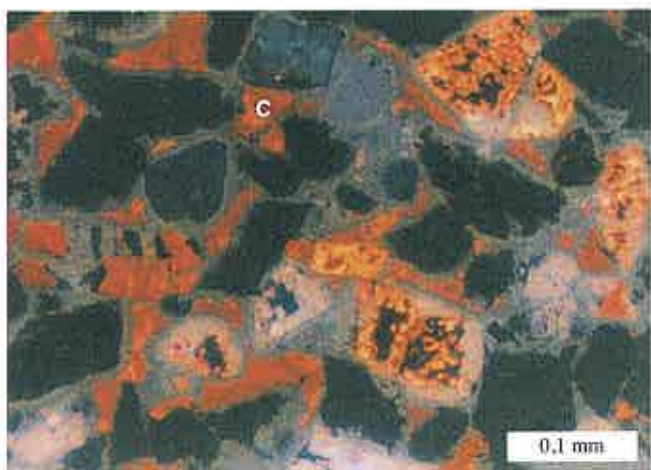


Fig. 7



Fig. 8



Fig. 9

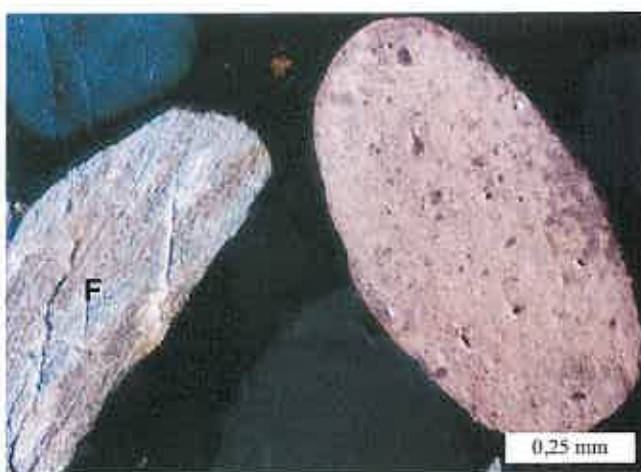


Fig. 10

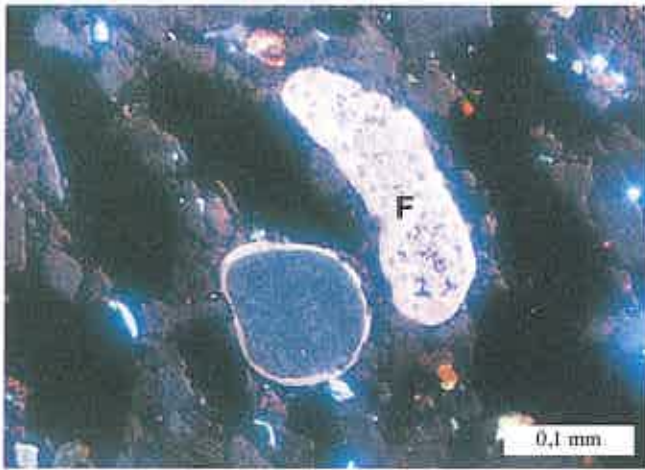


Fig. 11

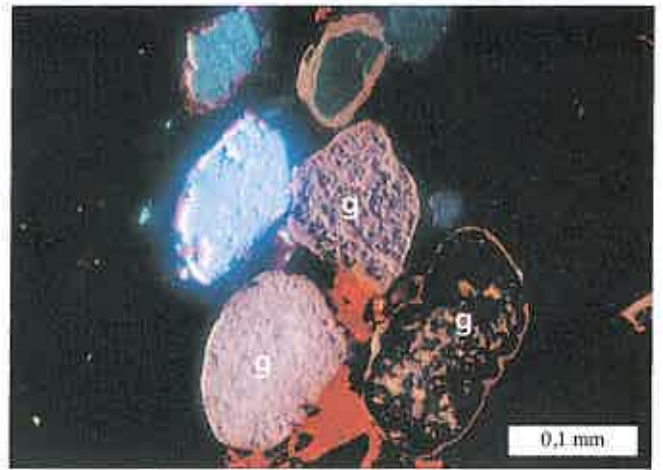


Fig. 12

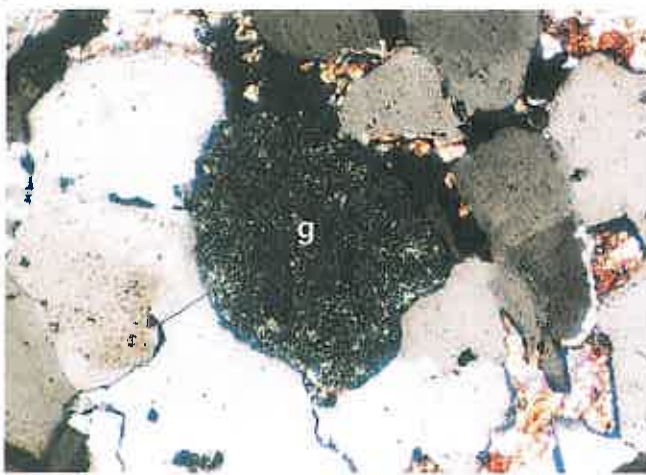


Fig. 13

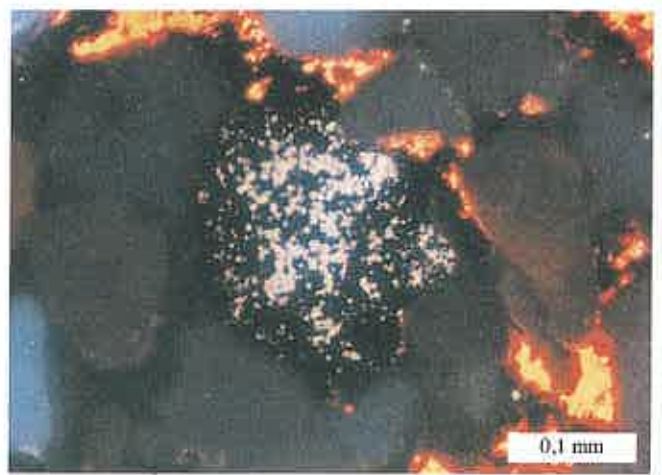


Fig. 14

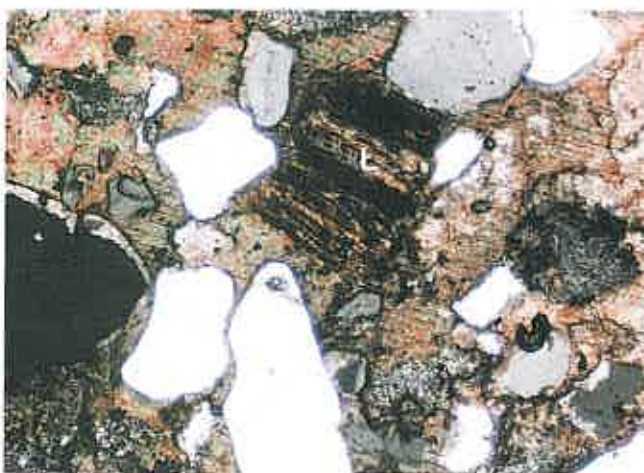


Fig. 15



Fig. 16

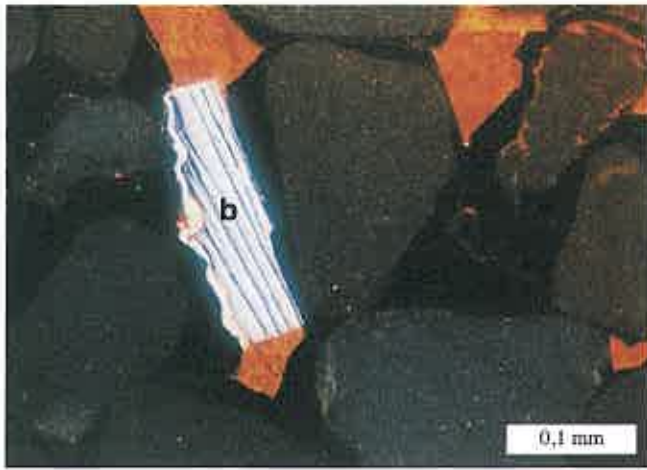


Fig. 17



Fig. 18

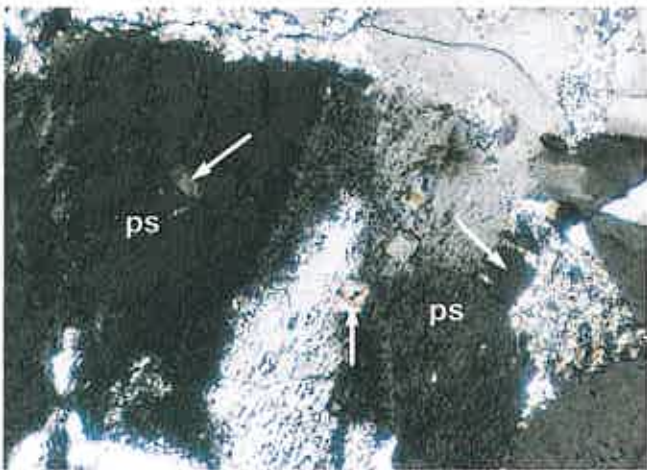


Fig. 19



Fig. 20

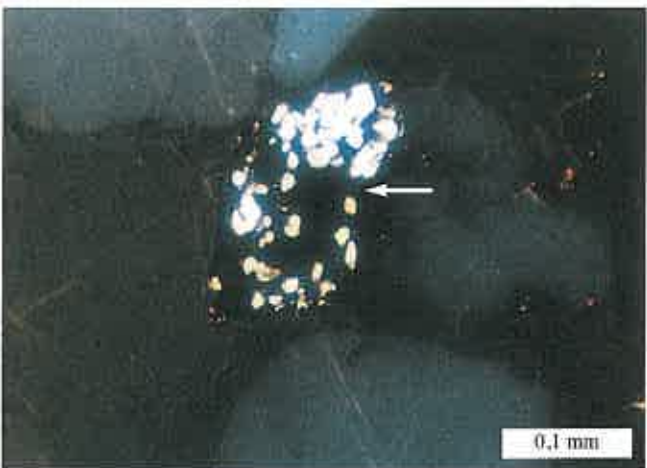


Fig. 21

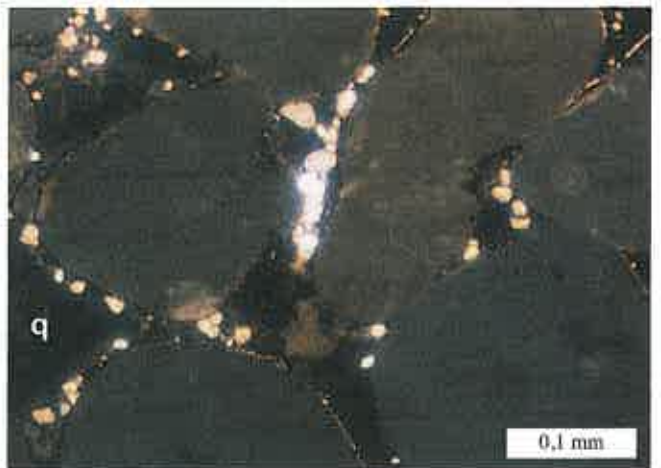


Fig. 22

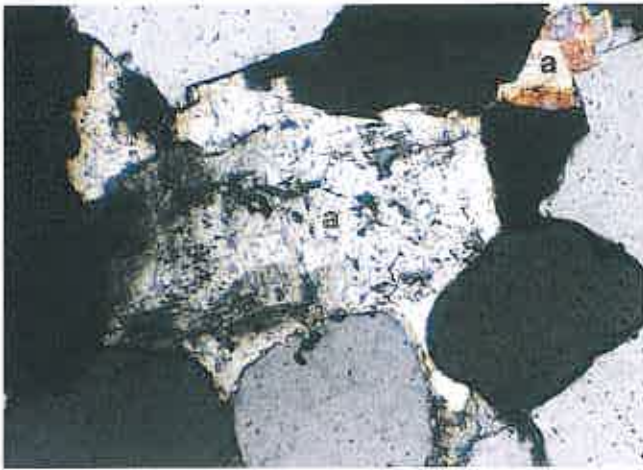


Fig. 23

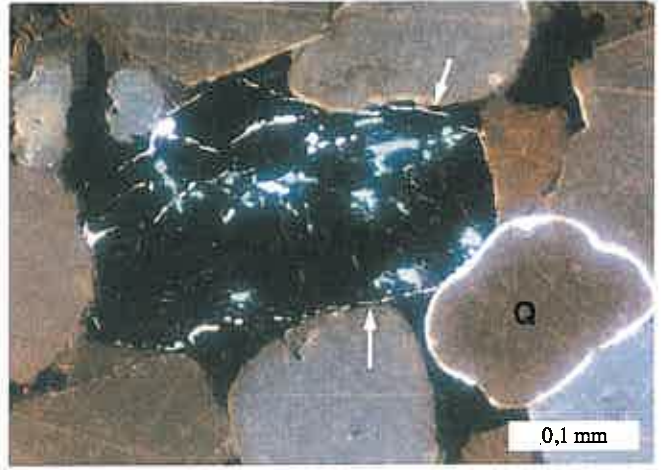


Fig. 24



Fig. 25

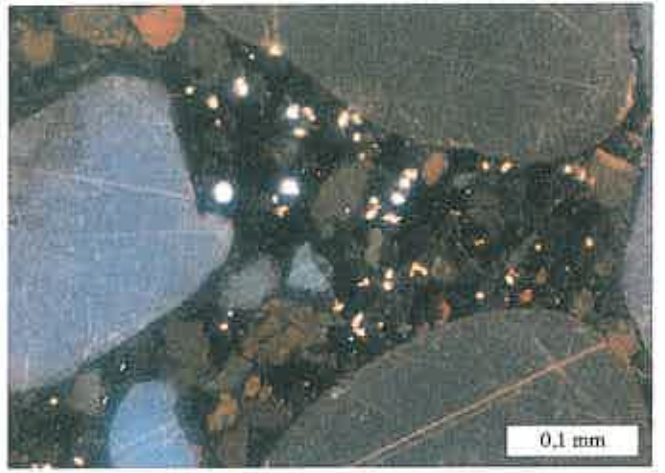


Fig. 26



Fig. 27

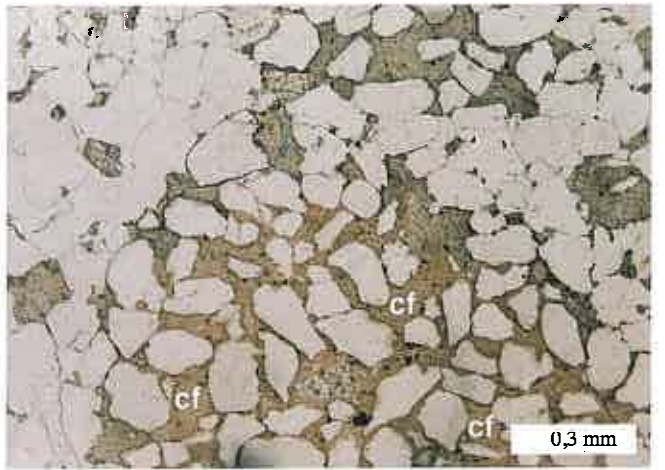


Fig. 28

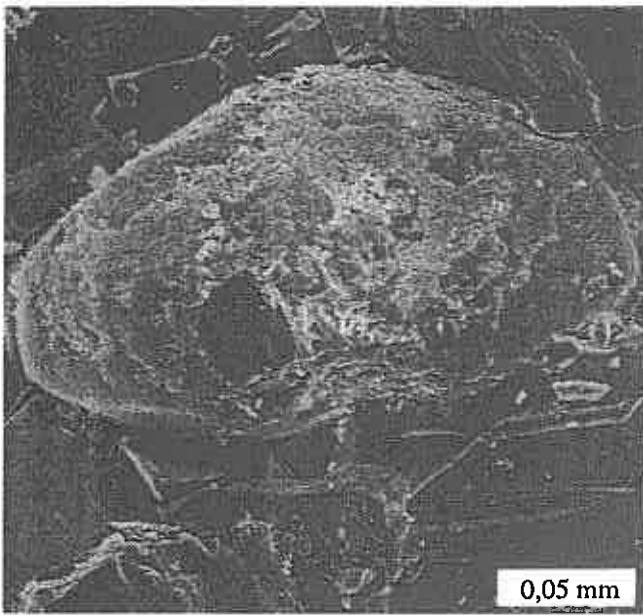


Fig. 29

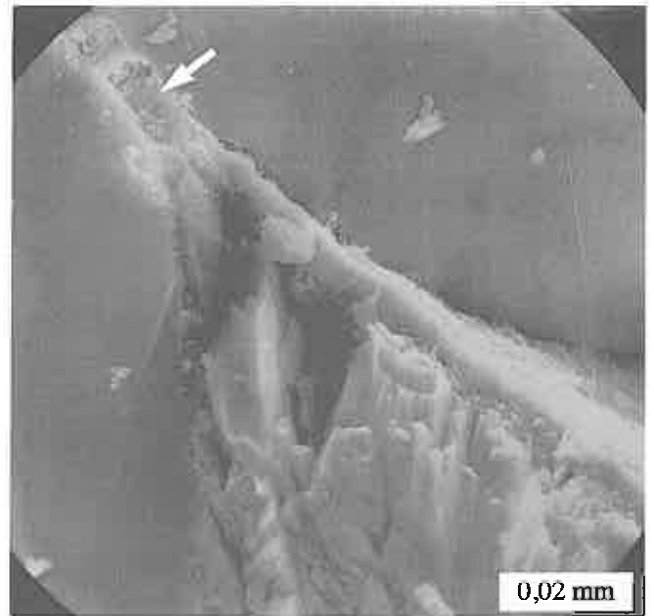


Fig. 30

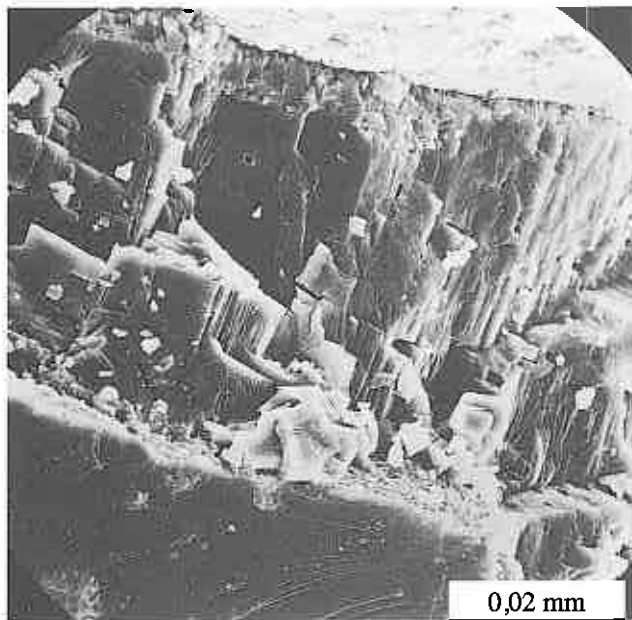


Fig. 31

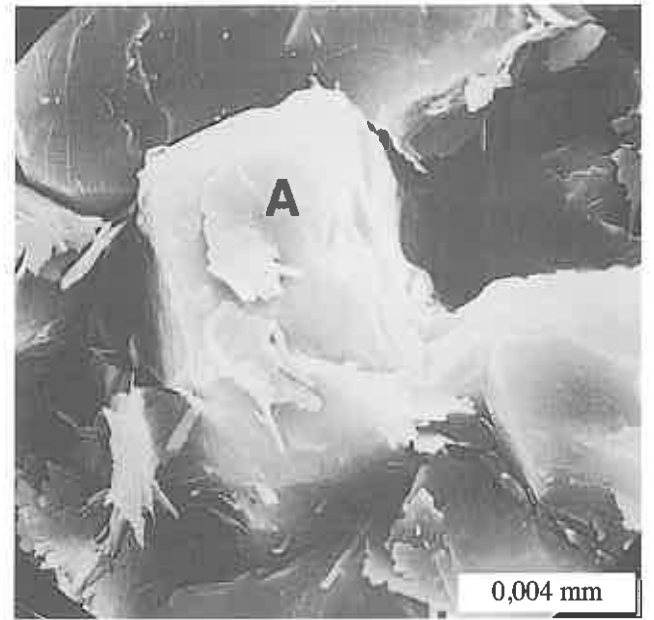


Fig. 32